PAPER • **OPEN ACCESS**

Factors affecting stress distribution in wind turbine blade

To cite this article: Diaaeldin M Elsherif *et al* 2019 *IOP Conf. Ser.: Mater. Sci. Eng.* **610** 012020

IOP Conf. Series: Materials Science and Engineering **610** (2019) 012020 doi:10.1088/1757-899X/610/1/012020

Factors affecting stress distribution in wind turbine blade

Diaaeldin M Elsherif[1,4], Ayman A Abd El-Wahab[2], Mohamed Hazem Abdellatif[3]

Ain Shams University, Faculty of Engineering, Mechanical Design and Production Engineering Department
[1]M.Sc. Student,
[2]Associate Professor,
[3]Professor

[4] Email. diaa.elsherif@msn.com

Abstract. In this study three factors affecting stress distribution in horizontal axis wind turbine blade are studied using ANSYS Fluid-Structure Interaction (FSI) simulation. The first factor is the cross-section of the wind turbine blade which is selected to be an airfoil. The second factor is the twist angle of the blade while the third factor is the material. A study of two different airfoils is made for three different blades' twist angles and two different materials to obtain the results of total deformation, stress distribution and maximum equivalent stress (von-Mises) along the blade length. This study emphasizes the importance of a multi-disciplinary research where computer, mechanics, and materials engineering are involved. The fields Computational Mechanics, Mechanical Design and Materials Engineering are used in the analysis of wind turbine blade in this study. Also understanding in depth the stress distribution in wind turbine blades could improve the design of wind turbines and lessen the cost of the clean wind energy.

1. Introduction

Any Computational Fluid Dynamics (CFD) simulation or Finite Element Analysis (FEA) is generally composed of pre-processing, processing, and post-processing. In the pre-processing the geometry is modelled, the mesh is generated, and the boundary conditions are defined. In the processing, the solution is computed while in the post-processing results are obtained, [6] and [7].

Fluid-Structure Interaction simulation is composed of two main parts. The first part is a computational fluid dynamics (CFD) simulation of the fluid flow around the blade to get the pressure load acting on the blade due to wind. The second part is a finite element analysis (FEA) of the blade to get the deformation and stress distribution due to pressure load and blade rotation. CFD is concerned with the fluid only while FEA is concerned with the solid blade shell. In the FEA, the blade is modelled as a shell with a web along the blade. The shell and the web thicknesses are getting thinner linearly from the base to the tip of the blade to get a lighter structure, [3] and [4].

2. Methodology

A fluid-structure interaction (FSI) computer simulation is made using ANSYS Software for each model of the horizontal axis wind turbine blade of 41 m length using two different materials which are Aluminum Alloy and Epoxy E-Glass Uni-Directional (UD), [3], [4], and [21]. The CFD, FEA, and FSI methodologies are discussed briefly in this study since FSI is used as a tool only to achieve the goal of studying the factors affecting the stress distribution in the wind turbine blade. The wind speed and the rated rotational speed are selected to be 12 m/s and 2.22 rad/s respectively [3]. The pitch angle which is the angle between the rotor plane (the plane of rotation) and the airfoil's chord line, [3], is 6 degrees at the root of the blade. While, the angle of attack is measured with the relative wind direction not the free stream wind direction. The angle of attack varies along the blade as the tangential velocity is dependent on the radius and this affects the relative wind direction.

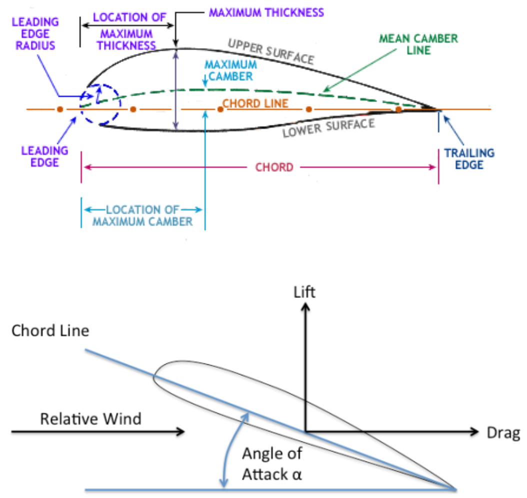

Figure 1. Airfoil terminology and positive angle of attack definition, [13] and [14]

The angle of attack is defined in figure 1 which is the angle between the relative wind vector and the chord line of the airfoil.

The properties of the modelled Epoxy E-Glass UD and the modelled Aluminum Alloy are listed in table 1 and 2 respectively.

In this study, each material is represented by its properties as mere numerical values of density, Young's modulus, Poisson's ratio, and shear modulus. The idea behind this is that numerical simulation deals with materials numerically and we can insert any custom material to the simulation by inserting the numerical values of its properties to the program. However, matweb.com could be searched to find the designation of the used Aluminum Alloy which is "Aluminum 5456-H24" available for purchase from alibaba.com website. Also the Epoxy E-Glass UD material designation from matweb.com is "APCM DA 4518U/E-Glass Unidirectional" which is available for purchase from prepregs.com.

The standard airfoils used in this study are NACA2412 and NACA2421, from National Advisory Committee for Aeronautics (NACA) which was founded in 1915 by Congress in the USA, as shown in figures 2 and 3 [5].

The selection of the airfoil NACA2412 was made because of its possible use in case of low Reynold's number while the selection of NACA2421 was made to have a greater maximum thickness compared to NACA2412. So the maximum thickness parameter was changed from 12% to 21%.

The airfoil code represents the max camber, max camber position and the thickness of the airfoil as shown in figure 1. These items are listed in table 3 for NACA2412 as an example.

Seven simulated models were selected to be analyzed in this study as listed in table 4.

Table 1. Epoxy E-Glass UD Material Properties, [2]

Property	Epoxy E-Glass UD	Unit
Density	2E-09	mm^-3 t
Young's Modulus X direction	45000	MPa
Young's Modulus Y direction	10000	MPa
Young's Modulus Z direction	10000	MPa
Poisson's Ratio XY	0.3	
Poisson's Ratio YZ	0.4	
Poisson's Ratio XZ	0.3	
Shear Modulus XY	5000	MPa
Shear Modulus YZ	3846.2	MPa
Shear Modulus XZ	5000	MPa
Stress Limits:		
Tensile X direction	1100	MPa
Tensile Y direction	35	MPa
Tensile Z direction	35	MPa
Shear XY	80	MPa
Shear YZ	46.1538	MPa
Shear XZ	80	MPa
Strain Limits:		
Tensile X direction	0.0244	
Tensile Y direction	0.0035	
Tensile Z direction	0.0035	
Shear XY	0.016	
Shear YZ	0.012	
Shear XZ	0.016	

Table 2. ANSYS Material Library Aluminum Alloy Material Properties, [2]

Property	Aluminum Alloy	Unit
Density	2770	kg m^-3
Young's Modulus	71000	MPa
Poisson's Ratio	0.33	
Bulk Modulus	69608	MPa
Shear Modulus	26692	MPa
Yield Strength	280	MPa
Tensile Ultimate Strength	310	MPa

Table 3. NACA2412 interpretation of each digit, [5]

Property	Value
Max Camber (%)	2
Max camber position (%)	40
Thickness (%)	12

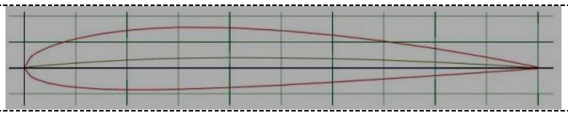

Figure 2. NACA2412 airfoil with chord of unit length

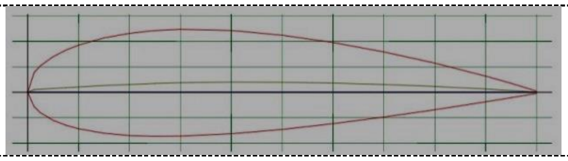

Figure 3. NACA2421 airfoil with chord of unit length

Table 4. Specifications of the simulated models

Model no.	Model Designation	Twist Angle [deg.]	Material	Blade Mass [kg]
1	NACA2412-0A	0	Al Alloy	197
2	NACA2412-3A	3	Al Alloy	198
3	NACA2412-3C	3	Epoxy E-Glass UD	143
4	NACA2412-6A	6	Al Alloy	199
5	NACA2412-6C	6	Epoxy E-Glass UD	144
6	NACA2421-0A	0	Al Alloy	215
7	NACA2421-0C	0	Epoxy E-Glass UD	155

In table 4, the first section of the model designation represents the airfoil standard which is selected to be either NACA2412 or NACA2421. The second section is the twist angle which is selected to be 0, 3, or 6 degrees. The last section indicates the material of the blade which is either Aluminum Alloy designated by A or Epoxy E-Glass Uni-Directional (UD) designated by C. For example, NACA2412-3C is a blade with NACA2412 airfoil and 3 degrees twist angle using Epoxy E-Glass UD. Another example is NACA2421-0A which is a straight blade (zero twist angles) of NACA2421 airfoil, and the blade material is Aluminum Alloy.

The geometry sections were modelled as shown in figure 4 then skin loft was applied to generate a shell based on the four cross-sections as shown in the figure. The generated shell has a variable thickness along its length. It linearly decreases from 0.1 m at the base of the blade to 0.005 m at the tip of the blade as shown in figure 5. On the other hand, the thickness of the web was varied linearly along its length from 0.1 m at the base of the blade to 0.03 m at the tip of the blade as shown in figure 6.

A straight blade with the combination of several airfoils or even a blade with a twist angle with two or three different airfoil cross-sections similar to wind turbine blades in [3] and [4] might cause modelling and manufacturing issues as the transformation from NACA2421 to NACA2412 in the geometry will result in a non-standard intermediate airfoil cross-sections which might be more expensive in its manufacturing. For having a simple concrete design one standard airfoil was used along the blade.

IOP Conf. Series: Materials Science and Engineering **610** (2019) 012020 doi:10.1088/1757-899X/610/1/012020

The rotation of the blade was represented by a rotating frame of reference around the positive z-axis of a value -2.22 rad/s. The frame of reference is the XYZ-coordinate system. In other words, 2.22 rad/s rated rotational speed of the three-bladed horizontal axis wind turbine clockwise was simulated.

Only one of the three blades was modelled and a periodic matching of the mesh was done. Periodic matching of the mesh is to model only a pie (one third of the rotor plane as shown in figure 8) including only one blade and adjust the mesh elements at the upper surface to match those elements in the lower surface. This achieves periodicity which compensates for modelling only one blade instead of three and adjusts the mesh in the pre-processing phase where mesh is generated then solving the problem in the processing phase. Finally in the post-processing phase, which is the last step of the CFD analysis, it has been possible to have the results of the three blades of the wind turbine.

The generated Computational Fluid Dynamics mesh is shown in figure 7 and figure 8 while the generated Finite Element Analysis mesh is shown in figure 9. These generated meshes are for NACA2412-0A.

In figure 7, the generated CFD mesh is done with face sizing and inflation options. Face sizing is used to define the size of the element to adjust the number of elements accordingly. While inflation option is used to have quadrilateral, rather than tetrahedral CFD mesh elements, at the boundary which is the surface of the blade. This resulted in 63794 nodes and 323249 elements.

Figure 8 represents an external view of the generated CFD mesh. The mesh size is fine at the blade and is coarse as getting away from the blade which is achieved by a sphere of influence. It has been used to adjust the mesh intensity to be higher as getting closer to the blade, which significantly reduces the computational cost of the simulation. This explains how this mesh is obtained.

In figure 9a, the FEA mesh is generated to be as uniform as possible resulting in slightly more than 4000 elements. The mesh metrics are shown in figures 9b and 9c for the mesh in figure 9a. It is noted that the mesh quality is very good since we have very high orthogonal quality and very low skewness. This reflects a uniform mesh.

The Fluid-Structure Interaction (FSI) simulation has to map the CFD mesh with much larger number of elements (323249 in this study) to the FEA mesh with a relatively small but sufficient number of elements (about 4000 elements). This mapping is the link between the CFD and FEA solutions which characterizes an FSI simulation and was successful using ANSYS by a percentage of 98%. The pressure load due to wind was successfully imported from the CFD simulation which was solved using a coupled solver with turbulence model using large deflections and pseudo transient solution which is a numerical modelling method, [3] and [4].

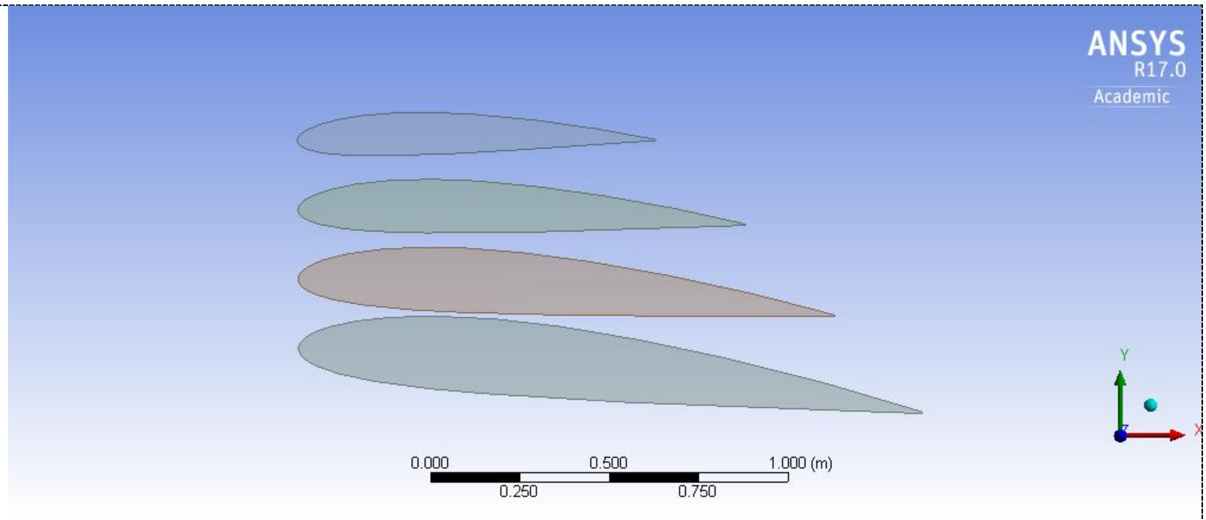

Figure 4. Wind Turbine Blade Geometry sections at the base, the tip and two intermediate sections

IOP Conf. Series: Materials Science and Engineering **610** (2019) 012020 doi:10.1088/1757-899X/610/1/012020

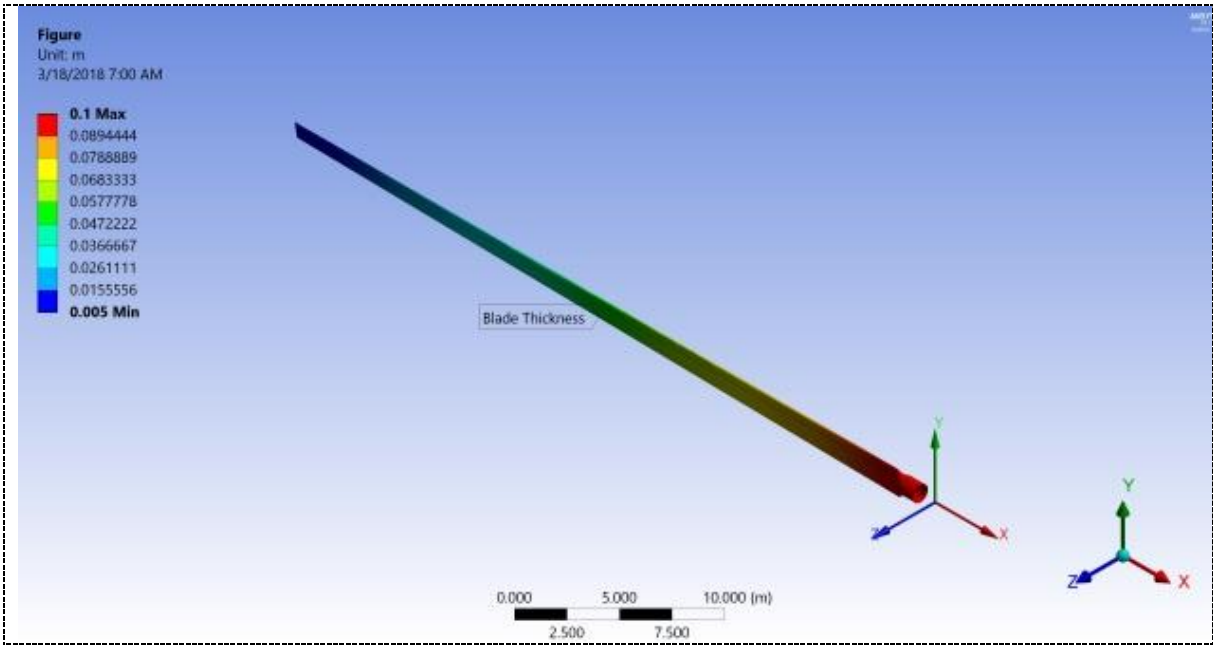

Figure 5. Wind Turbine Blade thickness along the blade length

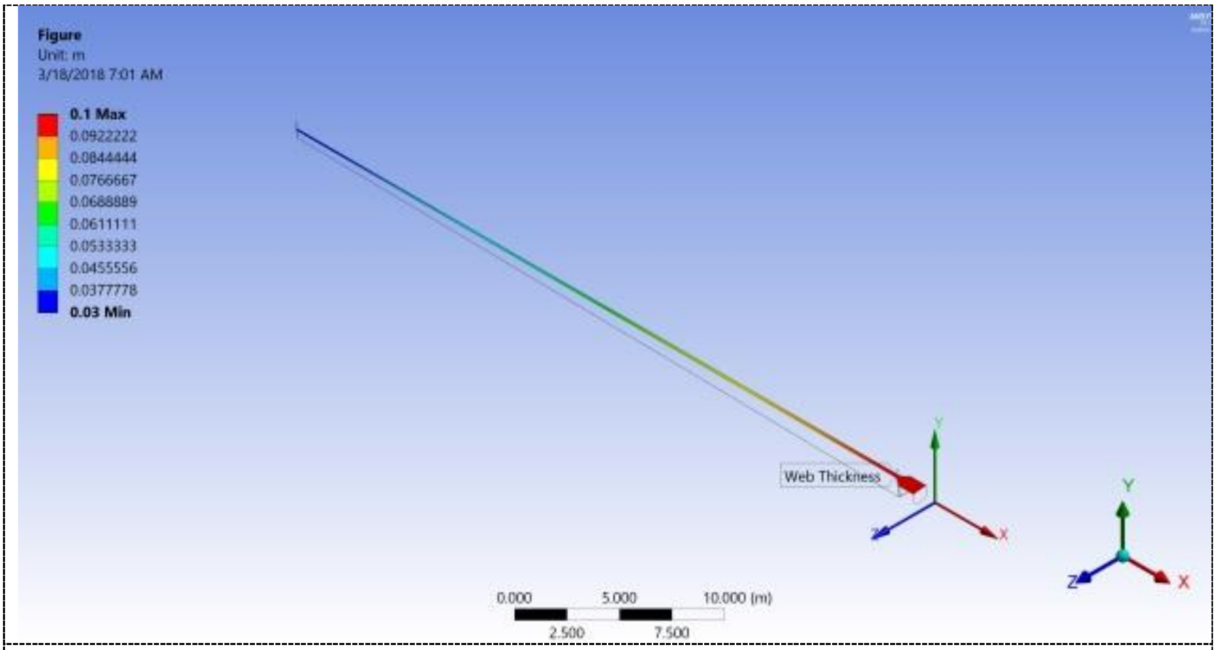

Figure 6. Wind Turbine Blade web thickness along the blade length

IOP Conf. Series: Materials Science and Engineering **610** (2019) 012020 doi:10.1088/1757-899X/610/1/012020

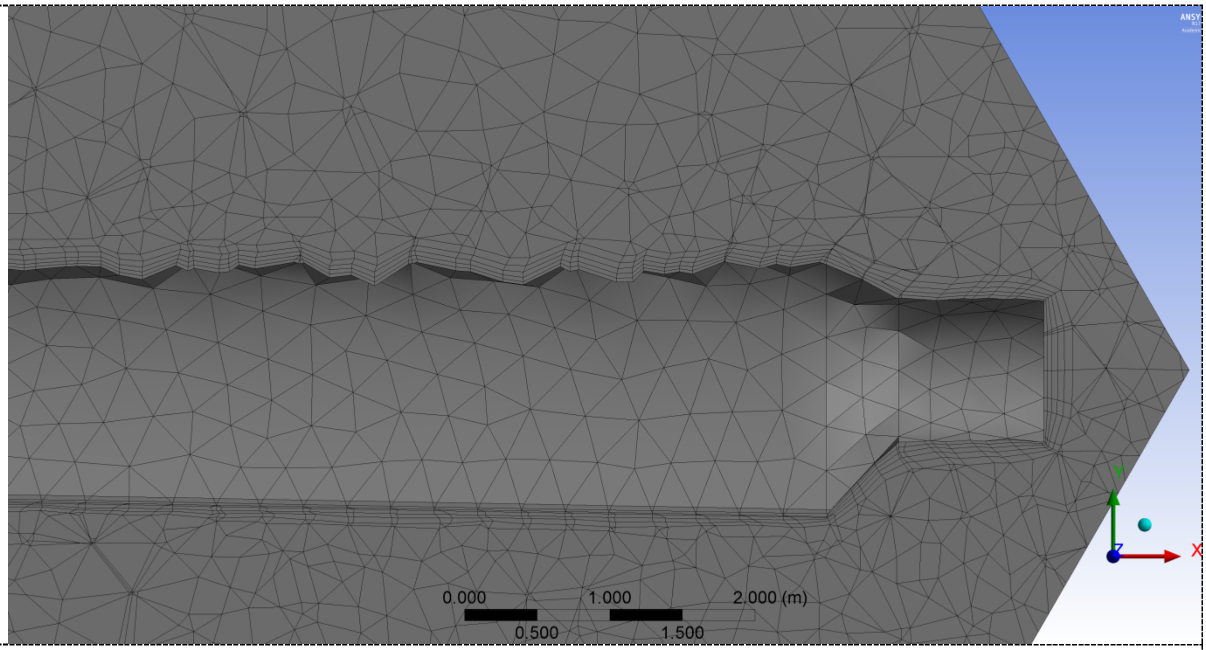

Figure 7. The Computational Fluid Dynamics (CFD) mesh cut in the XY-plane

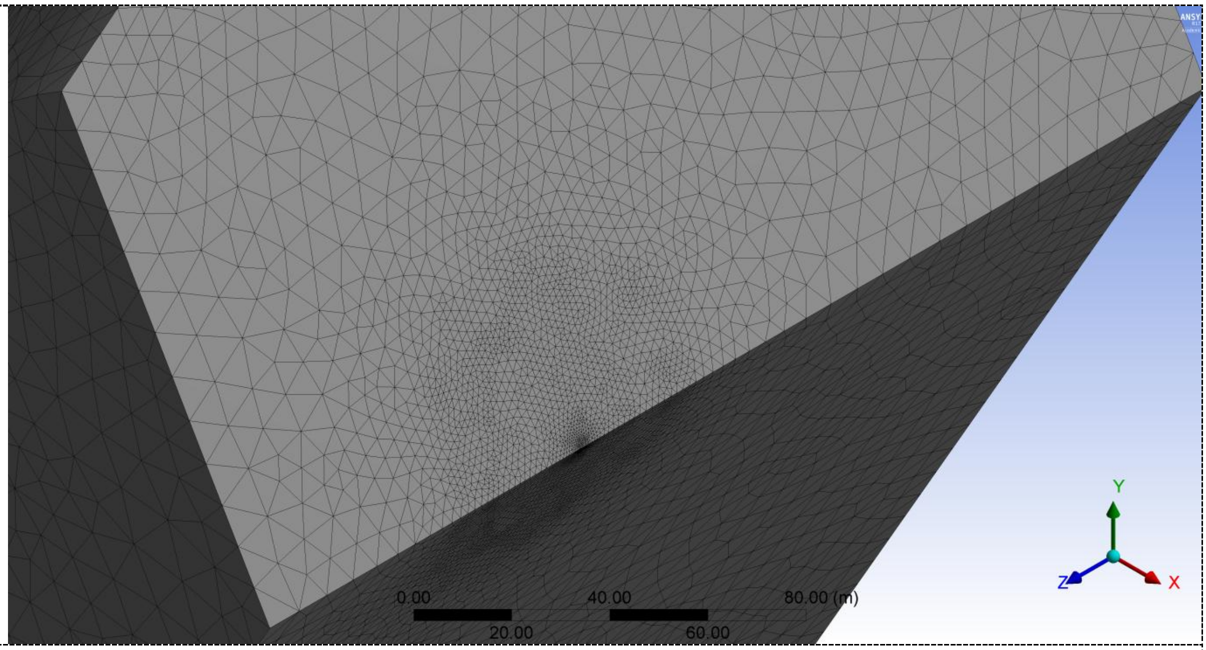

Figure 8. The Computational Fluid Dynamics mesh

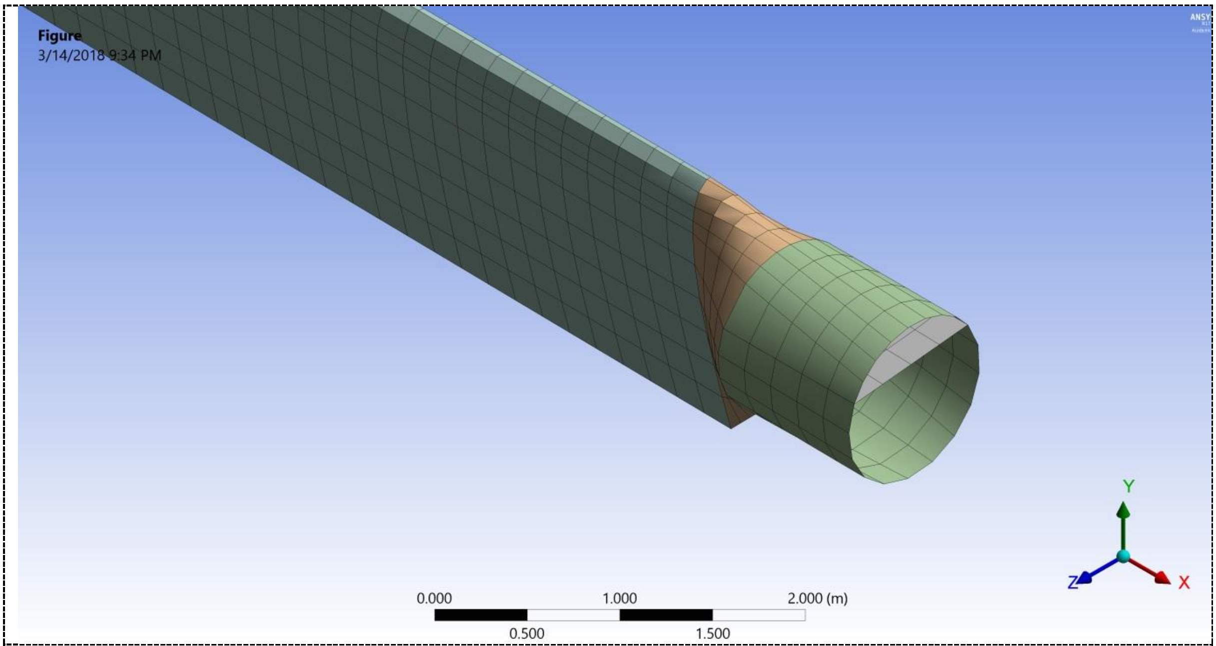

Figure 9a. The generated Finite Element Analysis (FEA) mesh (including mesh of the web inside the blade)

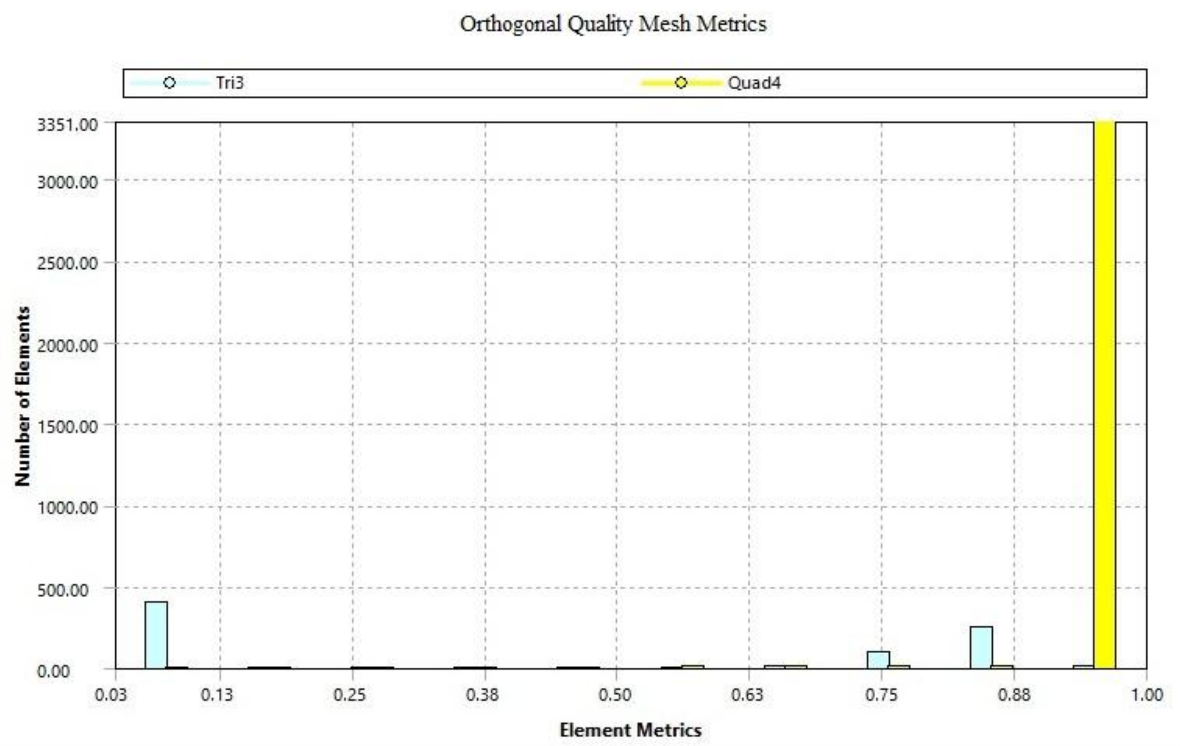

Figure 9b. The generated Finite Element Analysis (FEA) mesh orthogonal quality metrics

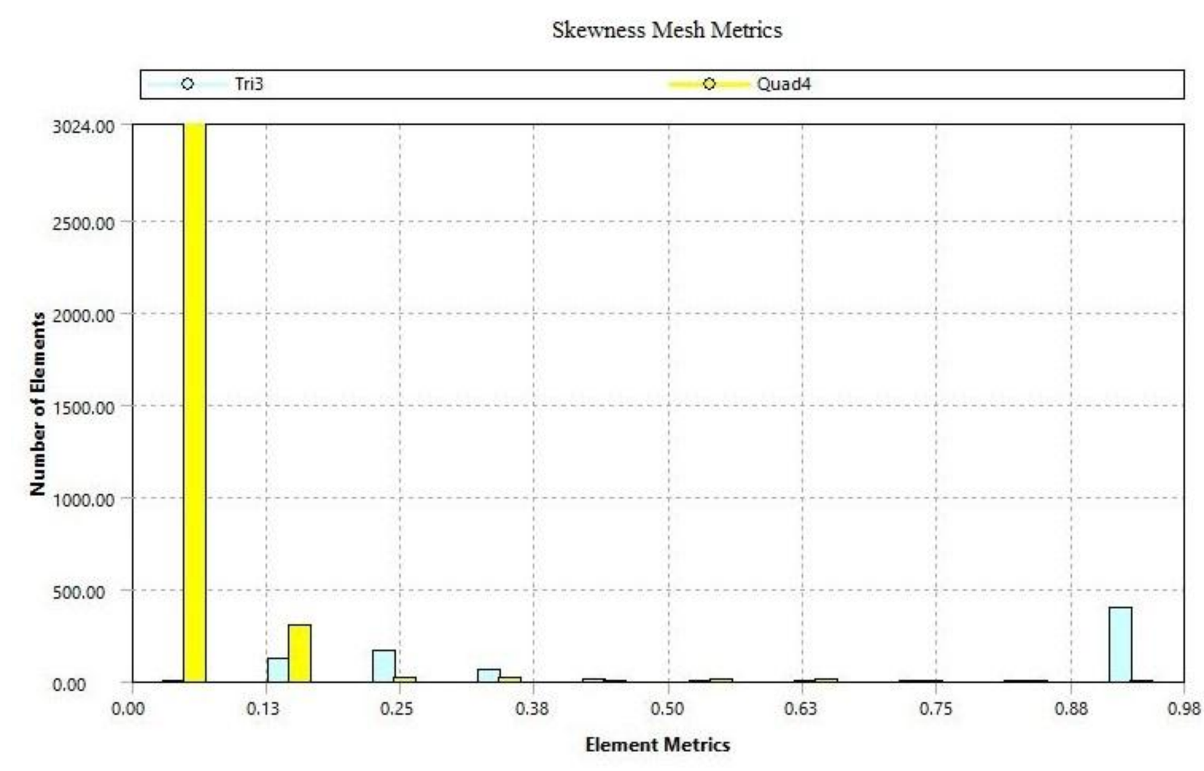

Figure 9c. The generated Finite Element Analysis (FEA) mesh skewness metrics

3. Results and Discussion

In this section, the results of the simulations applied to the seven models are analyzed and discussed.

In figure 10, the total deformation distribution in meters along the blade length is shown for model number 1 – NACA2412-0A. The maximum total deformation is at the tip of the blade and is about 1.29 m. This blade has airfoil cross section NACA2412 and its material has to be Aluminum Alloy or any homogenized isotropic alloy.

Figure 11 shows that the maximum equivalent (von-Mises) stress, 43.4 MPa, is at the base of the blade. Consequently, the material was selected to be Aluminum Alloy and Epoxy E-Glass UD was excluded because the von-Mises stress is larger than the stress limit of the Epoxy E-Glass UD which is 35 MPa in the y and z axes directions. This is may be due to the small value of pitch angle (6 degrees) which means large value of angle of attack or due to thin airfoil.

This resulted in failure of the Epoxy E-Glass UD for model number 1 so Aluminum Alloy was used instead (NACA2412-0A).

In figure 12, a twist angle of 3 degrees was introduced and a new model was created with pitch angle of 6 degrees at the base of the blade and 9 degrees at the tip of the blade. This resulted in having a maximum total deformation at the tip of the blade of 0.708 m.

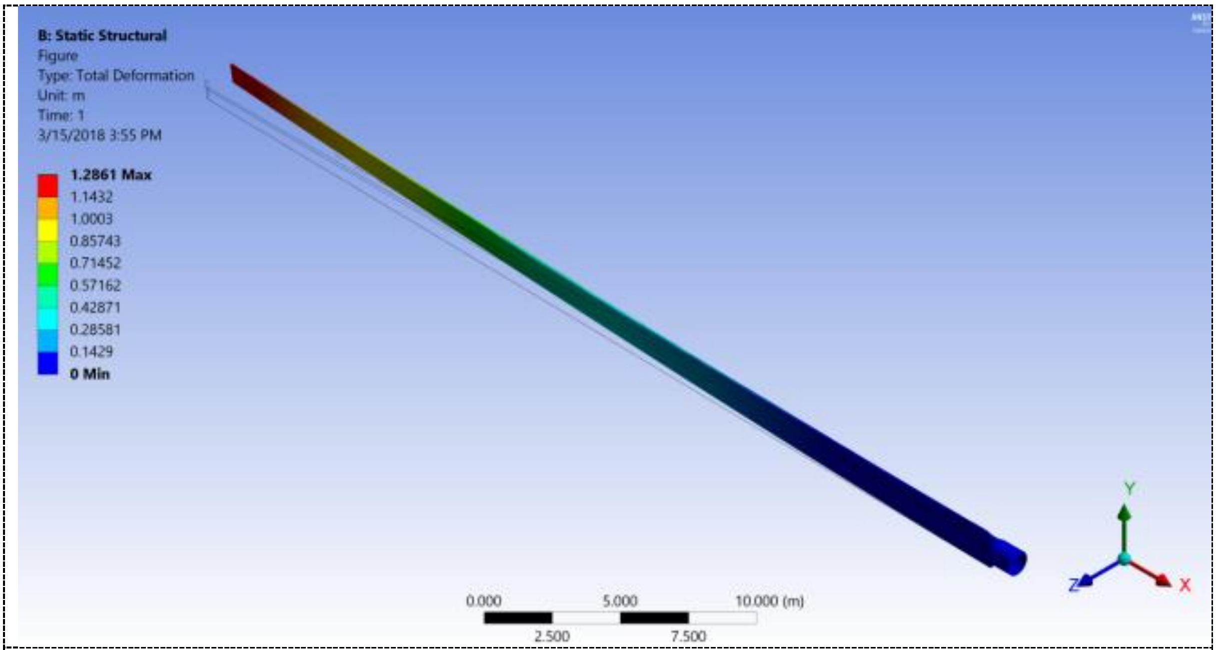

Figure 10. Total deformation distribution along the blade length for model number 1

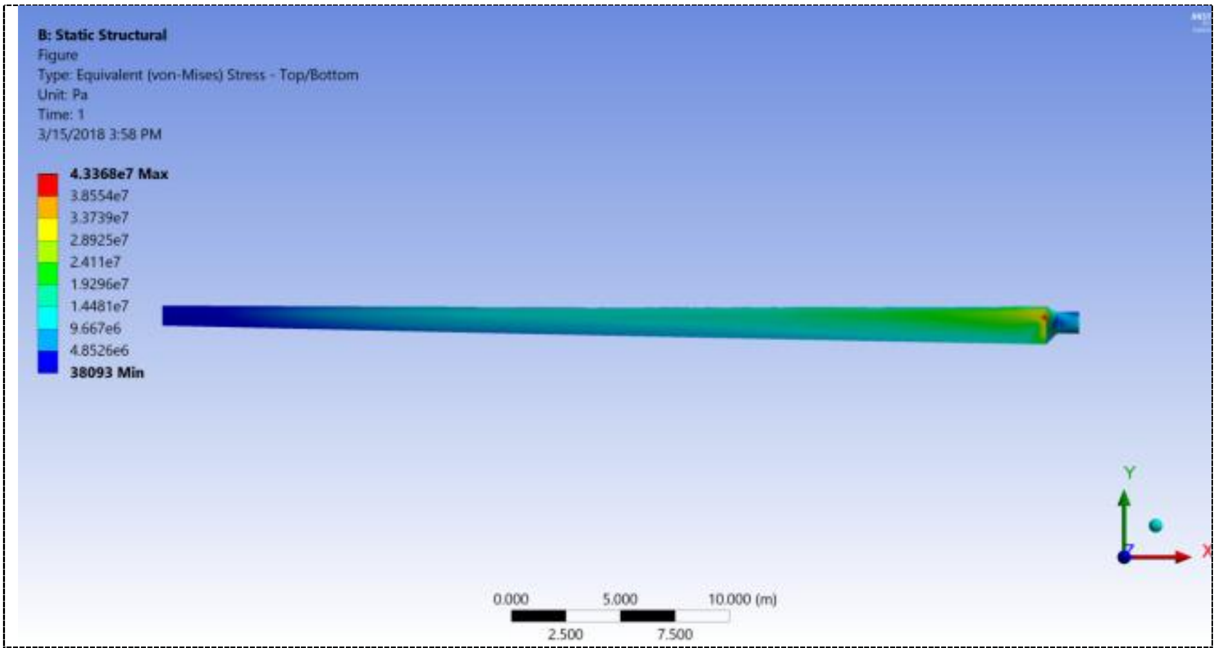

Figure 11. Equivalent (von-Mises) Stress distribution along the blade length for model number 1

IOP Conf. Series: Materials Science and Engineering **610** (2019) 012020 doi:10.1088/1757-899X/610/1/012020

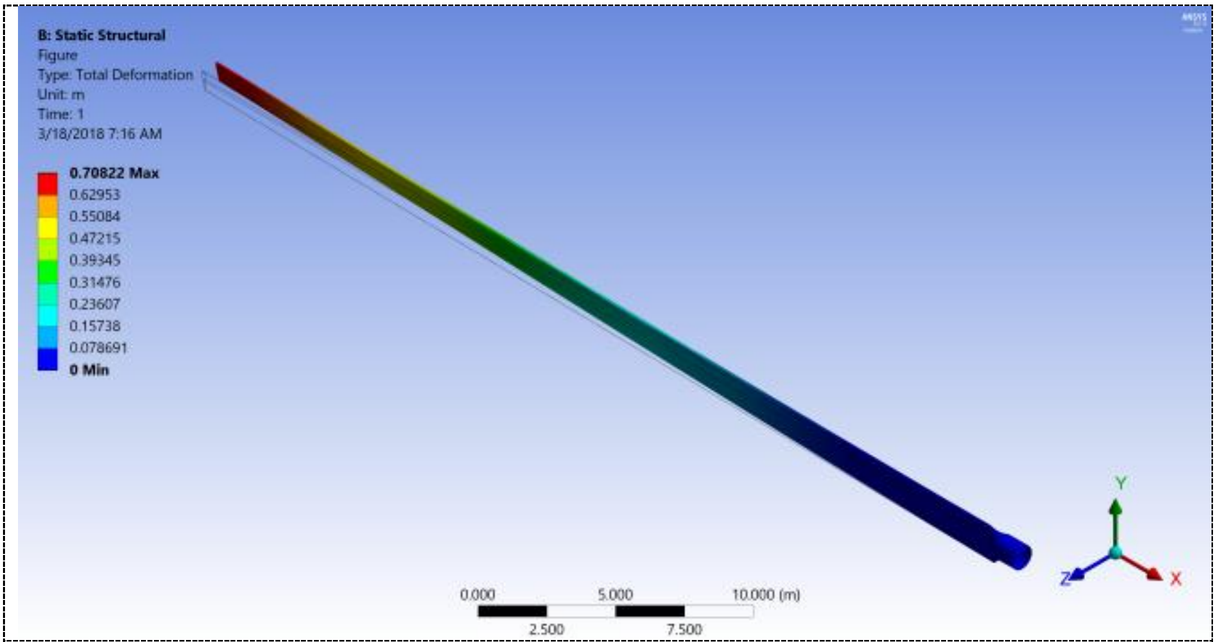

Figure 12. Total deformation distribution along the blade length for model number 2

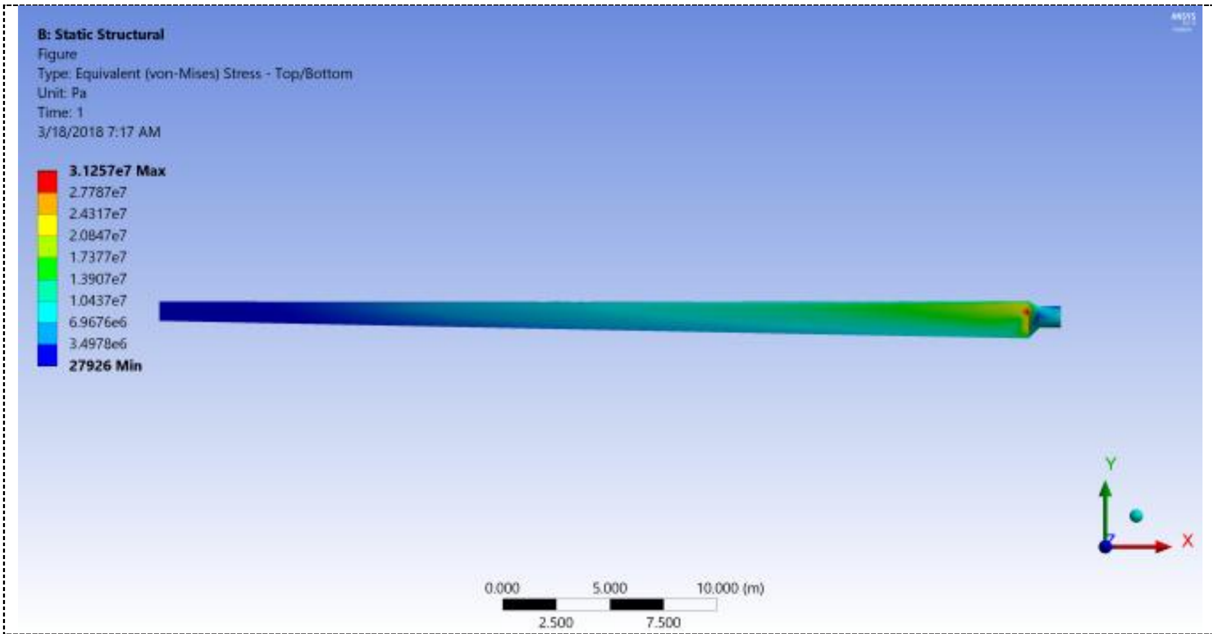

Figure 13. Equivalent (von-Mises) Stress distribution along the blade length for model number 2

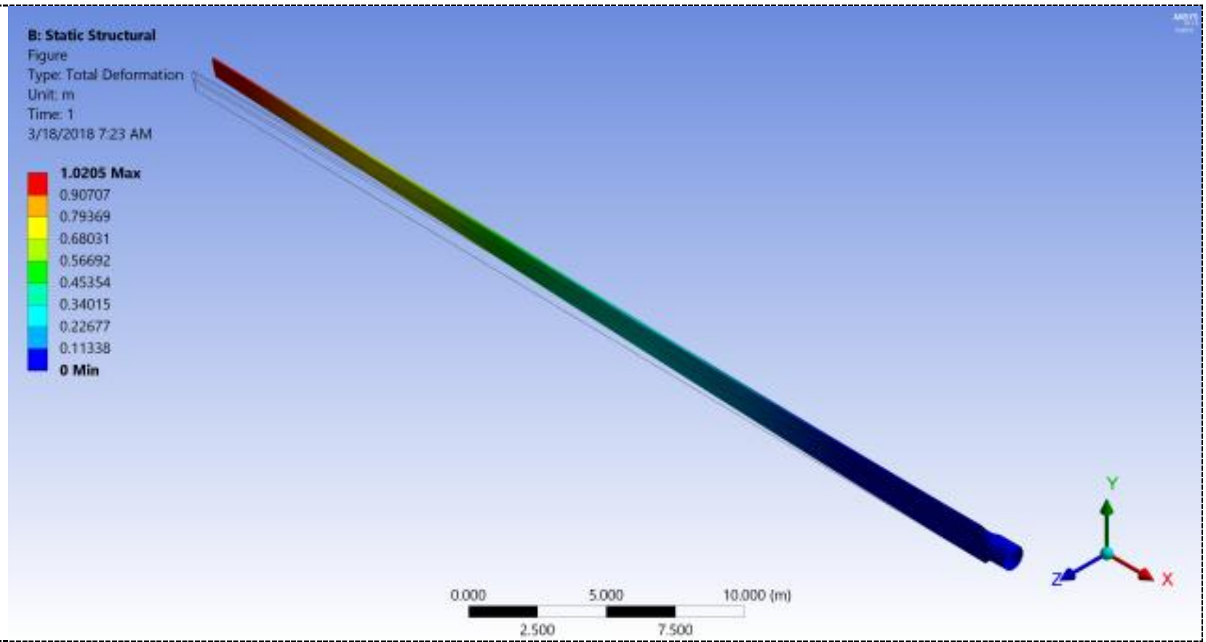

Figure 14. Total deformation distribution along the blade length for model number 3

In figure 13, von-Mises stress distribution for model number 2 – NACA2412-3A is shown. The maximum von-Mises stress is 31.3 MPa which is very safe when compared to the yield strength of the used material, so the same model geometry was used and the material was changed to be Epoxy E-Glass UD instead of Aluminum Alloy. These new results are for model number 3 which is a variant of model number 2 but with different material as mentioned above.

In figure 14, total deformation distribution along the blade is shown for model number 3. The maximum tip total deformation is 1.02 m.

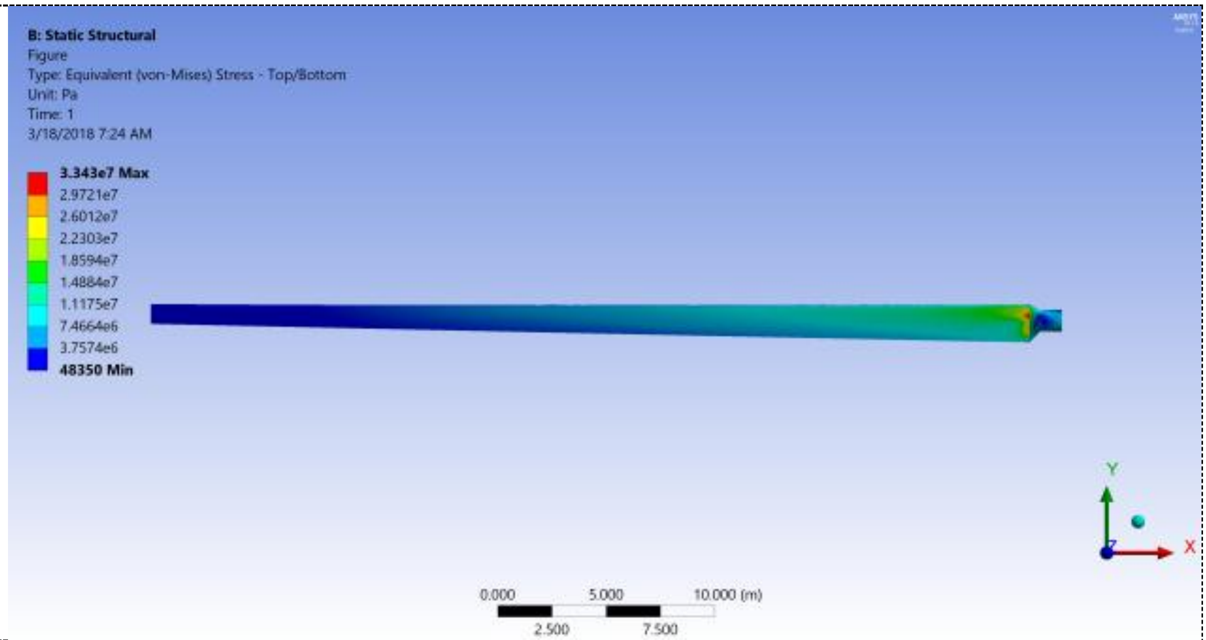

Figure 15. Equivalent (von-Mises) Stress distribution along the blade length for model number 3

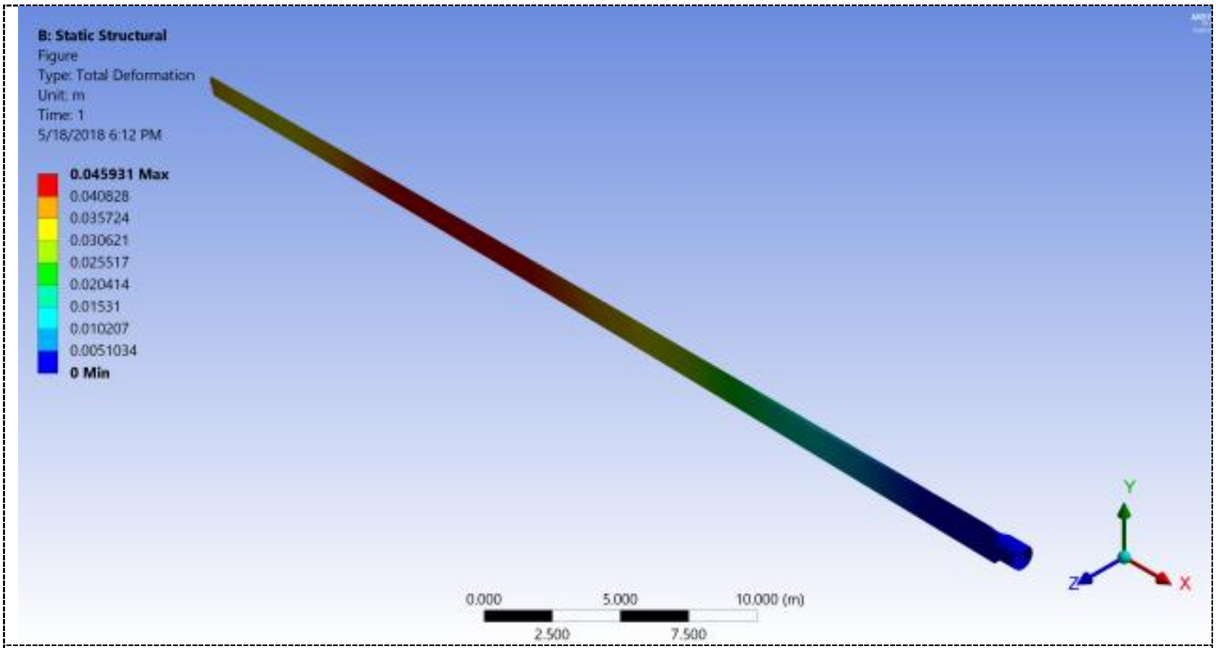

Figure 16. Total deformation distribution along the blade length for model number 4

The von-Mises stress distribution in the wind turbine blade of model number 3 is depicted in figure 15 where the maximum stress is 33.4 MPa which is lower than the stress limit of the Epoxy E-Glass UD (35 MPa). So, the design is safe.

Figure 16 shows the total deformation distribution along the blade for model number 4. The maximum total deformation is not at the tip due to the aerodynamics and the twist angle of the blade. The value of the maximum total deformation is 0.0459 m.

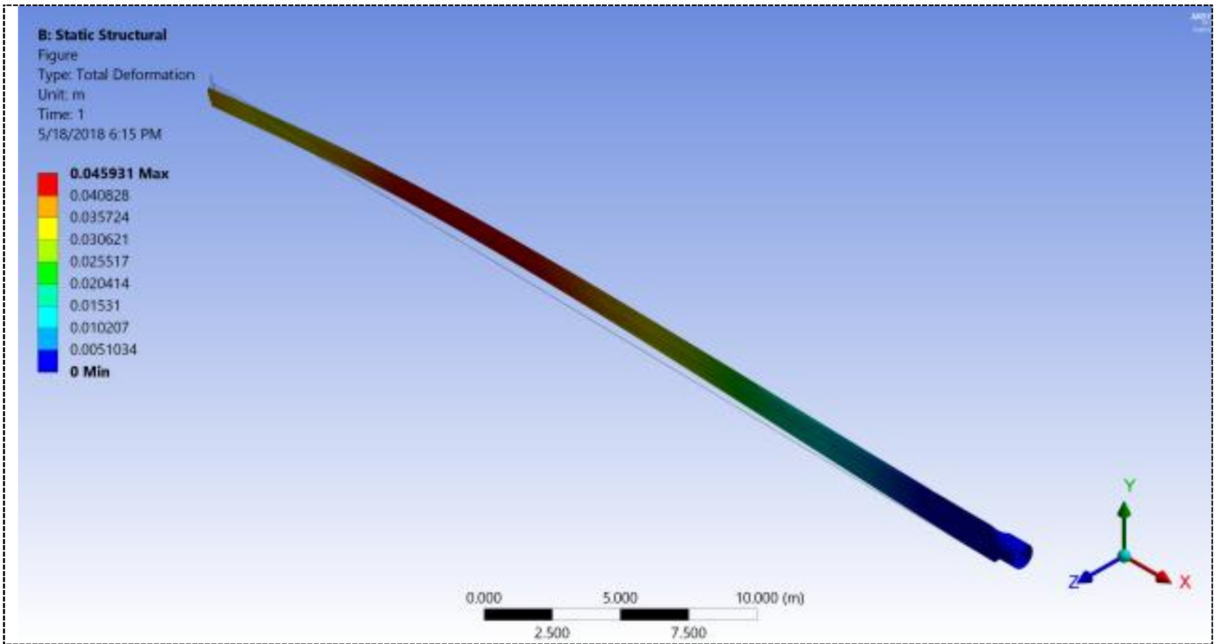

Figure 17. Total deformation distribution along the blade length for model number 4

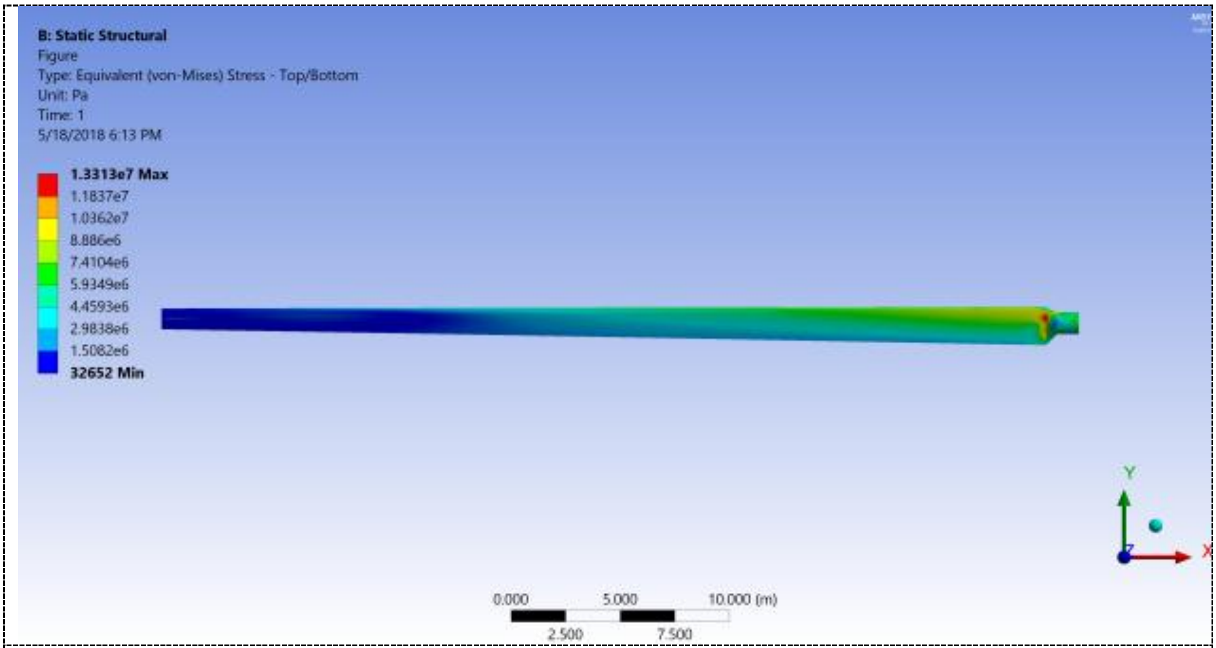

Figure 18. Equivalent (von-Mises) Stress distribution along the blade length for model number 4

In figure 18, the equivalent (von-Mises) stress distribution of model number 4 is shown. The maximum von-Mises stress is at the root of the blade, at the point where the web is fixed which is shown in red color. This resulted in stress concentration which could raise the grade of the material consequently using more expensive or even heavier material reducing the power output of the wind turbine. The value of the maximum von-Mises stress for this model obtained from the Fluid-Structure Interaction simulation done in this study is 13.3 MPa.

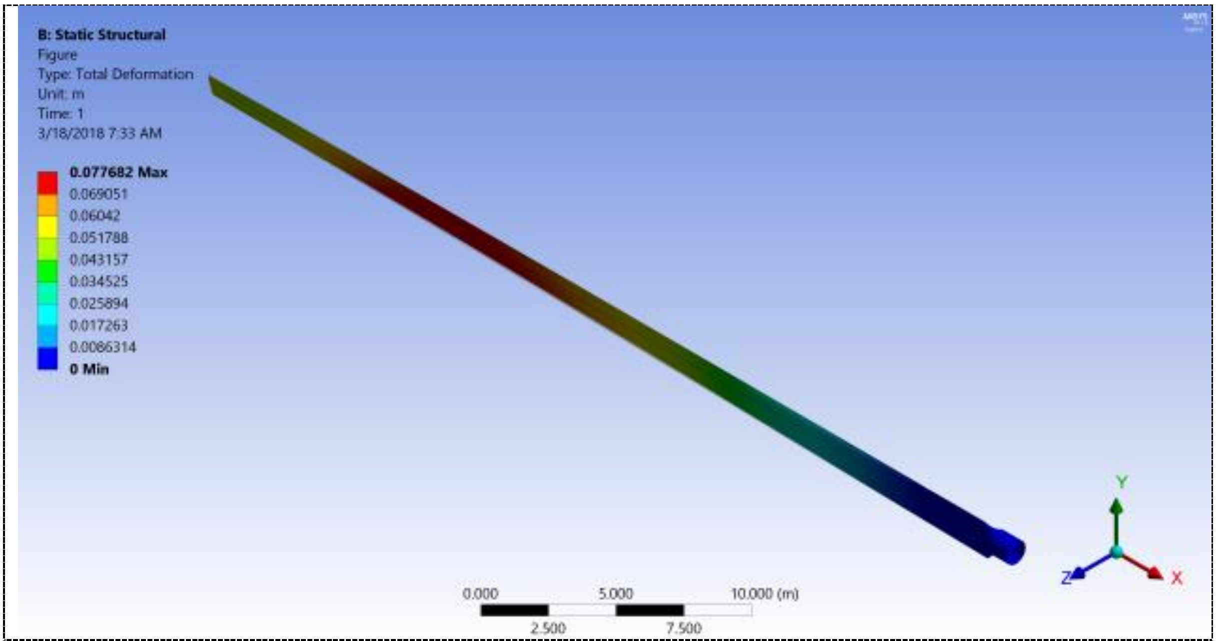

Figure 19. Total deformation distribution along the blade length for model number 5

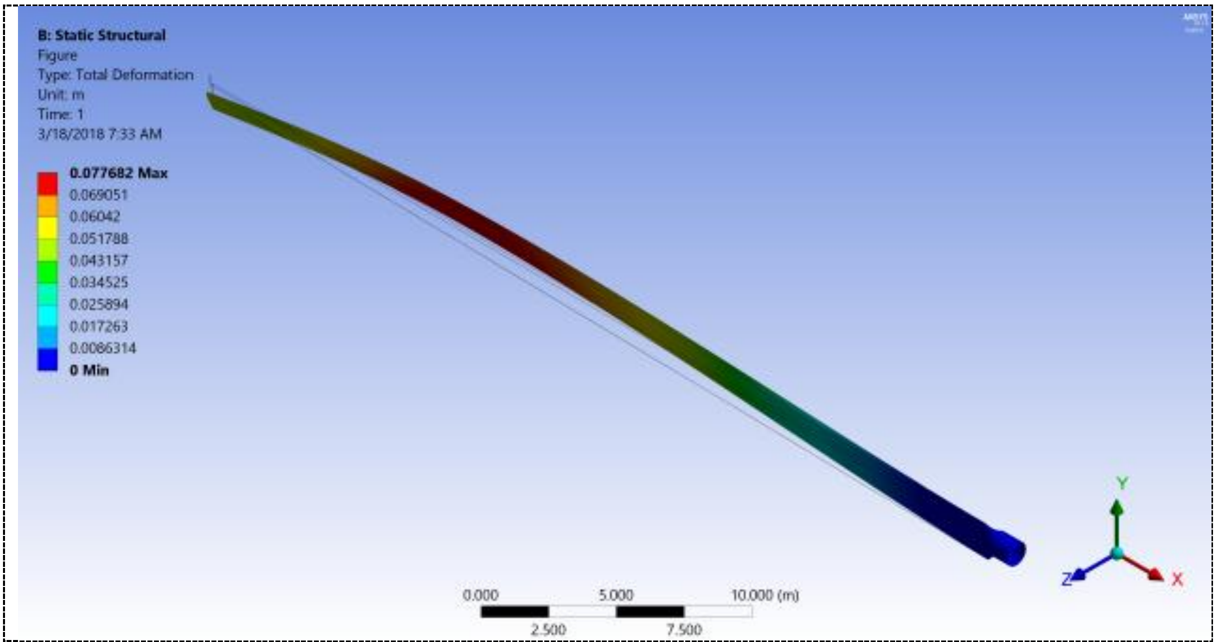

Figure 20. Total deformation distribution along the blade length for model number 5

Figure 19 shows the total deformation distribution along the blade for model number 5. The maximum total deformation is not at the tip due to the aerodynamics and the twist angle of the blade. The value of the maximum total deformation is 0.0777 m.

Figure 20 shows the same results of figure 19 but at 14x amplification factor to be able to see the twist clearly.

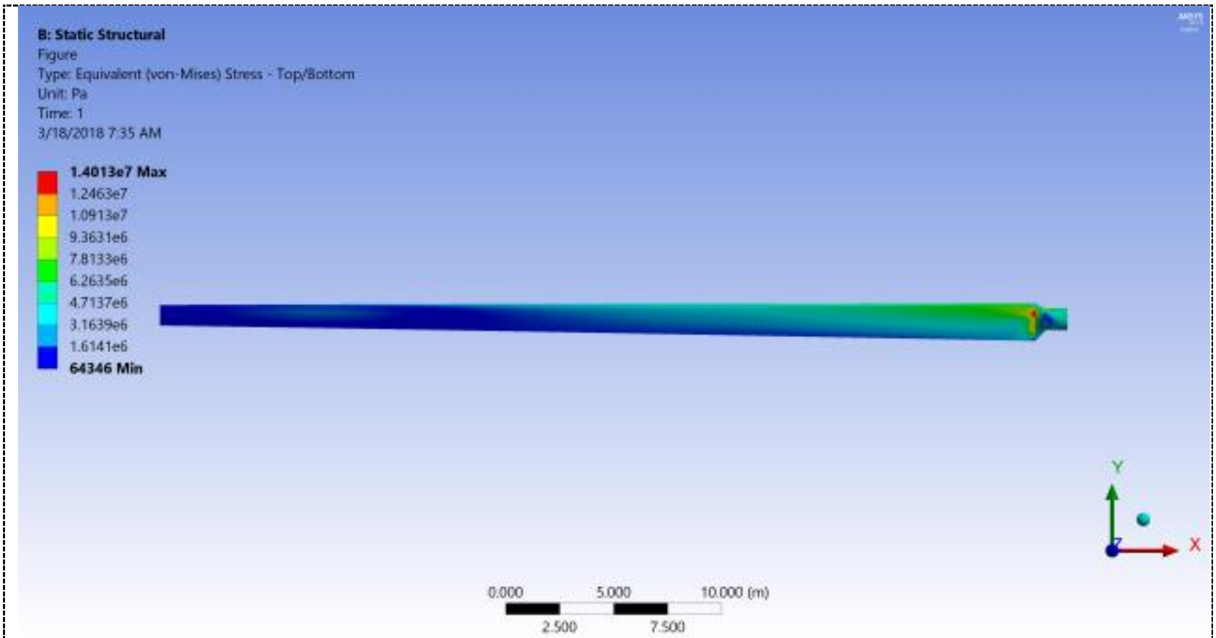

Figure 21. Equivalent (von-Mises) Stress distribution along the blade length for model number 5

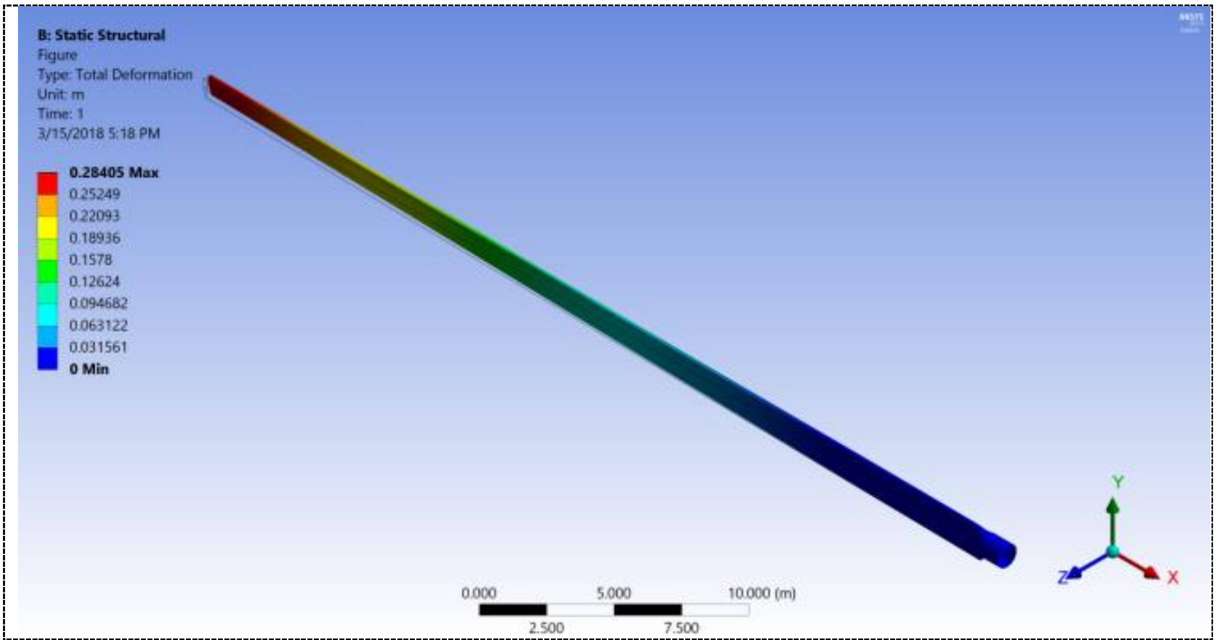

Figure 22. Total deformation distribution along the blade length for model number 6

In figure 21, the equivalent stress distribution for the blade model number 5 is depicted. The figure shows that the maximum stress is at the root of the blade with value of 14 MPa which is much lower than the stress limits of the Epoxy E-Glass UD.

Figure 22 shows the total deformation distribution of model number 6. The straight blade with NACA2421 airfoil is much stronger than that one with NACA2412 airfoil because NACA2412 has a smaller maximum thickness. For model number 6 the material is Aluminum Alloy which results in a total deformation of 0.284 m at the tip of the blade.

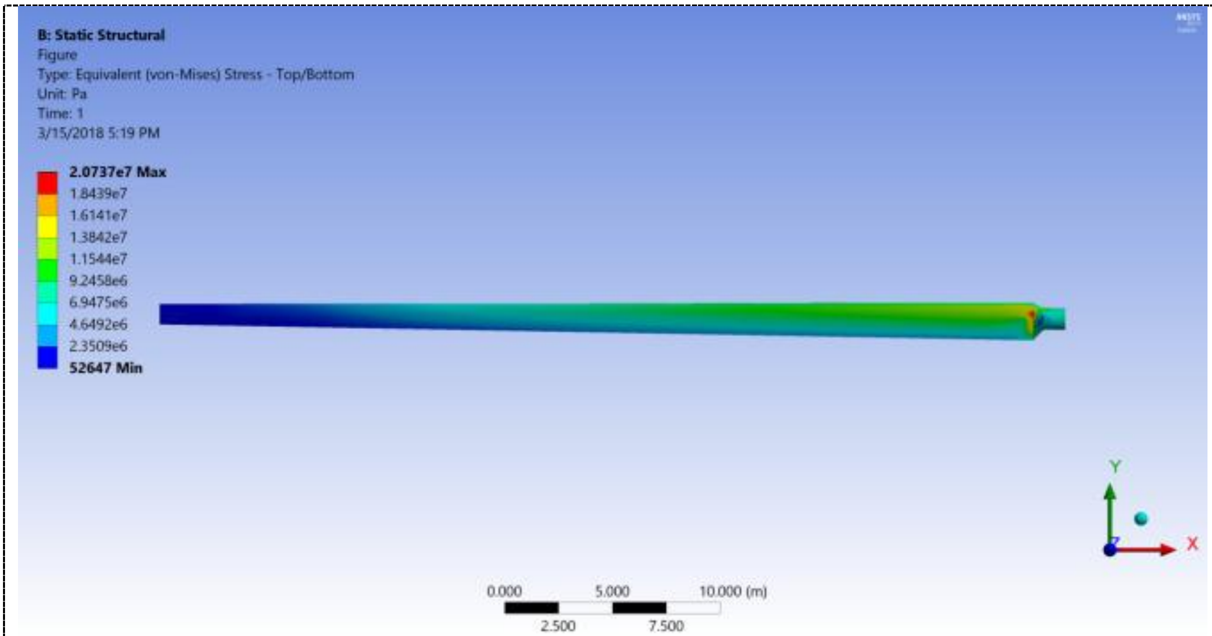

Figure 23. Equivalent (von-Mises) Stress distribution along the blade length for model number 6

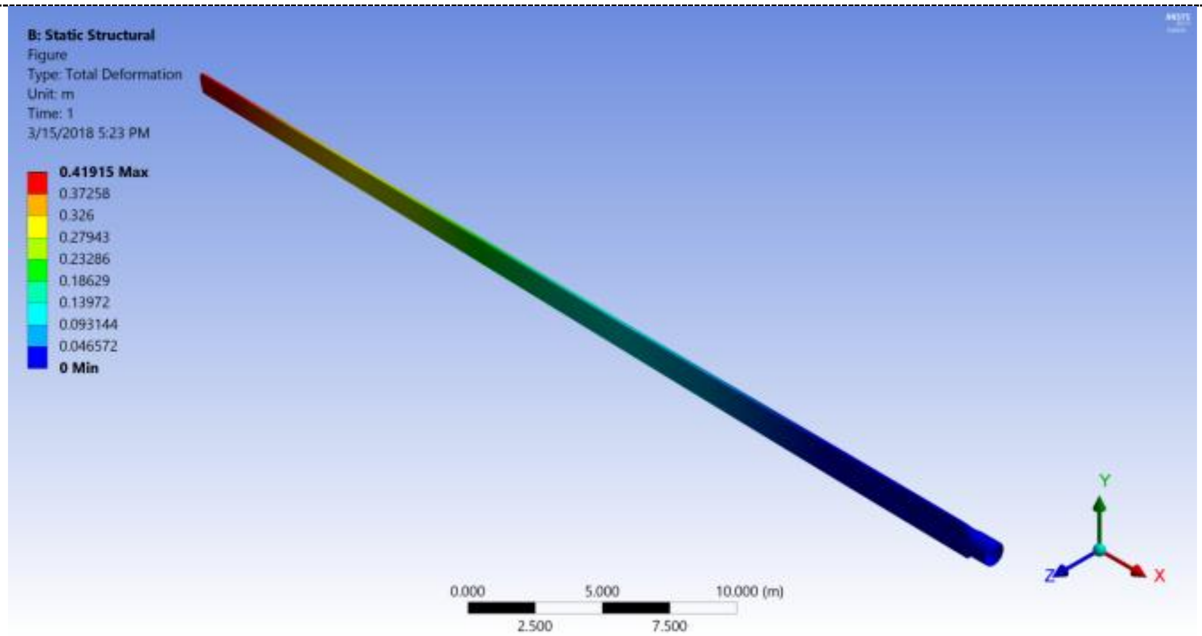

Figure 24. Total deformation distribution along the blade length for model number 7

In figure 23, the equivalent stress distribution of the blade is shown for model number 6. The maximum value of the von-Mises stress at the base of the blade is 20.7 MPa.

Total deformation distribution of model number 7 is shown in figure 24. It also shows that the maximum tip total deformation is 0.419 m.

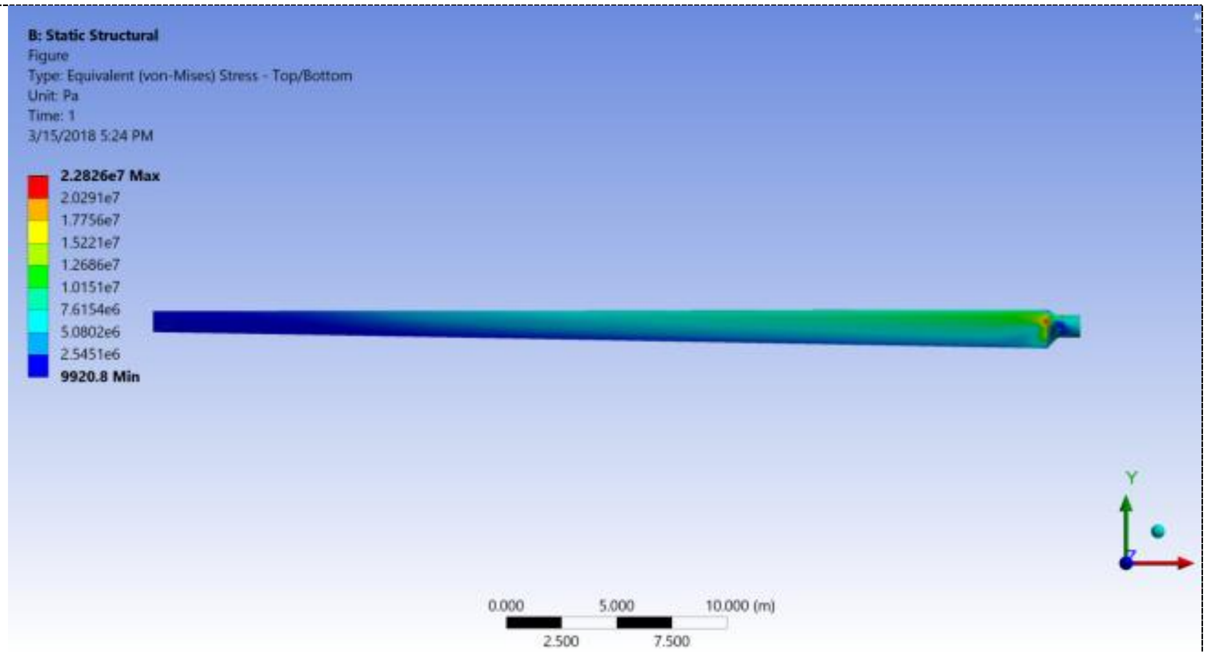

Figure 25. Equivalent (von-Mises) Stress distribution along the blade length for model number 7

Figure 25 shows the equivalent stress distribution along the blade for model number 7. It shows that the value of the maximum von-Mises stress will be at the base of the blade and is equal to 22.8 MPa.

IOP Conf. Series: Materials Science and Engineering **610** (2019) 012020 doi:10.1088/1757-899X/610/1/012020

Since the accuracy of the results of the numerical simulation depends on several aspects which includes the capabilities of the computer used, supercomputers are required for very accurate results where a supercomputer is a computer that performs at or near the currently highest operational rate for computers, [12]. Also the Fluid-Structure Interaction Simulation (FSI) is iterative in nature where several runs should be made to achieve very accurate results. This is a single run simulation. Also the finer the mesh the better the results but computational cost will significantly increase and sometimes it is not possible to solve an extremely fine mesh with limited capabilities and limited computer operational speed. Consequently, model 6 could be preferred to model 7 from the point of design safety.

The case study results of maximum total deformation and maximum von-Mises stress for each model are listed in table 5.

Table 5. Case Study Maximum Total Deformation and Maximum Equivalent Stress (von-Mises) for Each Model

	Model	Maximum Total Deformation [m]	Maximum Equivalent Stress (von-Mises) [MPa]
1	NACA2412-0A	1.29	43.4
2	NACA2412-3A	0.708	31.3
3	NACA2412-3C	1.02	33.4
4	NACA2412-6A	0.0459	13.3
5	NACA2412-6C	0.0777	14
6	NACA2421-0A	0.284	20.7
7	NACA2421-0C	0.419	22.8

4. Conclusion

Seven different models are simulated using Fluid-Structure Interaction (FSI) simulation to evaluate the stress and the deformation for a wind turbine blade along its length. This will help in continuous modifications in blade parameters to improve blade design.

As for NACA2412-6A and NACA2412-6C (models no. 4 and 5), they are rejected or has to be modified because part of the blade close to the tip will resist the rotation of the wind turbine. The blade part which has positive angle of attack from the root of the blade till the point of maximum total deformation will cause the blade to accelerate while the part from that point to the tip of the blade will cause the blade to decelerate reducing power output because of the fact that the angle of attack is negative in the latter as depicted in figures 17 and 20. This conclusion will lead us to reject these models or shorten the blade and correct the design. So 6 degrees twist angle is too large under these conditions of wind speed of 12 m/s and blade length of 41 m. Another modification to accept these models is to change the pitch angle at the base of the blade but this will lead to new values of stress and strain. So we would have to simulate the modified design in order to design using Fluid-Structure Interaction (FSI) simulation. This gives us a deeper insight of the aerodynamics, stress distribution and total deformation of the horizontal-axis wind turbine blade.

As for the two models NACA2412-3C and NACA2421-0C (models number 3 and 7), the design is safe and light as the material used is Epoxy E-Glass UD (Uni-Directional) with designation "APCM DA 4518U/E-Glass Unidirectional". For model number 7 the design is safe as the stress limits in the y and z directions of 35 MPa is higher than the maximum von-Mises stress for the designed blade which is 22.8 MPa. Moreover, the simulated maximum total tip deformation is found to be 0.419 m for a blade of total rotor diameter 42 m. For NACA2412-3C (model number 3) the design is also safe as the stress limits of the material 35 MPa is higher than the maximum von-Mises stress of 33.4 MPa. Also the simulated maximum total tip deformation is 1.02 m which is acceptable as the blade will not fail.

As for NACA2421-0A (model no. 6) when compared to NACA2421-0C (model no. 7), it is found that model no. 7 is preferred to model no. 6 as the material is lighter which will improve the performance of the wind turbine.

IOP Conf. Series: Materials Science and Engineering **610** (2019) 012020 doi:10.1088/1757-899X/610/1/012020

Finally, NACA2412-0A and NACA2412-3A (models no. 1 and 2) are both safe. Yet model no. 1 would give higher performance as the tip total deformation 1.29m is larger than that of model no. 2 which is 0.708m as this reflects that the wind pressure is larger on the blade due to the aerodynamics of the blade causing it to deform more. Also the maximum von-Mises stress reflects the same fact. So the straight blade is preferred to the twisted blade under the same conditions in our study as both materials are Aluminum Alloys designated “Aluminum 5456-H24”.

Comparing NACA2412-3C, NACA2421-0C, and NACA2412-0A (models no. 3, 7, and 1) gives us that NACA2412-3C (model no. 3) is the best model to be selected for manufacturing the wind turbine blade as its light weight would compensate for the difference in performance compared to the heavy NACA2412-0A (model no. 1). It is also felt from the results of maximum von-Mises stress that the aerodynamics of NACA2412-XX models is better for the wind turbine application than NACA2421-XX models.

References

[1] ANSYS® Academic, Release 17.0 Computer Software Tool with Academic License
[2] ANSYS® Academic, Release 17.0 Computer Software Material Library
[3] Sebastien Lachance-Barrett & Edwin Corona (2018, December). Wind Turbine Blade FSI Part 1. http://confluence.cornell.edu/pages/viewpage.action?pageId=262012971
[4] Sebastien Lachance-Barrett & Edwin Corona (2018, December). Wind Turbine Blade FSI Part 2. https://confluence.cornell.edu/pages/viewpage.action?pageId=262013005
[5] NACA 4 digit airfoil generator (2019). airfoiltools.com/airfoil/naca4digit
[6] Roland Wuechner (2009). Finite Element Method 1. Course at Technical University of Munich. https://www.bgu.tum.de/en/come/home/
[7] Michael Manhart (2011). Computational Fluid Dynamics. Course at Technical University of Munich. https://www.bgu.tum.de/en/come/home/
[8] Mechanical Design and Production Engineering. Courses at Ain Shams University. https://eng.asu.edu.eg/postgraduateProgram
[9] Kevin Cox and Andreas Echtermeyer 2012 Structural Design and Analysis of a 10MW Wind Turbine Blade, Energy Procedia **24**
[10] F. W. Perkins and Duane E. Cromack 1978 Wind Turbine Blade Stress Analysis And Natural Frequencies Technical Report (USA: University of Massachusetts)
[11] What is Von Mises Stress (2012). https://www.learnengineering.org/what-is-von-mises-stress.html
[12] What is supercomputer (2019). https://whatis.techtarget.com/definition/supercomputer
[13] Angle of Attack (2018). http://www.aviationchief.com/angle-of-attack.html
[14] Airfoil Terminology (2015, March). http://wwwaeroforum.blogspot.com/2015/03/air-foilterminology-air-foil-isprimary.html
[15] Nitin Tenguria, Mittal.N.D, and Siraj Ahmed 2010 Design and Finite Element Analysis of Horizontal Axis Wind Turbine blade, International Journal of Applied Engineering Research
[16] Meng-Kao Yeh and Chen-Hsu Wang 2017 Stress analysis of composite wind turbine blade by finite element method, ACMME
[17] Hao Wang*, Bing Ma, Jiaojiao Ding, Shuaibin Li 2014 The Modelling and Stress Analysis of Wind Turbine Blade, TELKOMNIKA Indonesian Journal of Electrical Engineering
[18] Mourad. NACHTANE, Mostapha. TARFAOUI, Dennoun. SAIFAOUI, Ahmed. EL MOUMEN 2018 Finite element analysis of composite wind turbine blade under the critical loads, Eleven International Conference on Thermal Engineering: Theory and Applications
[19] P.K. Nigam*, Nitin Tenguria, M.K. Pradhan 2017 Analysis of horizontal axis wind turbine blade using CFD, International Journal of Engineering, Science and Technology
[20] Lin Wang, Robin Quant and Athanasios Kolios* 2016 Fluid structure interaction modelling of horizontal-axis wind turbine blades based on CFD and FEA, Journal of Wind Engineering and Industrial Aerodynamics

IOP Conf. Series: Materials Science and Engineering **610** (2019) 012020 doi:10.1088/1757-899X/610/1/012020

[21] Diaaeldin M. Elsherif, Ayman A. Abd El-Wahab, Ramadan Badawy Mohamed Elgamsy, Mohamed Hazem Abdellatif 01/2019 Material Selection Of Wind Turbine Blade Using Finite Element Method, International Journal of Scientific & Technology Research **8** Issue 1